

## Short communication

## Low thermal expansion porous SiC–WC composite ceramics

Jifeng Pang, Jinping Li \*

*Department of Engineering Mechanics, Dalian University of Technology, No. 2 Linggong Road, Dalian 116024, China*

Received 5 June 2008; received in revised form 14 January 2009; accepted 6 May 2009

Available online 6 June 2009

**Abstract**

Low thermal expansion porous SiC–WC composite ceramics were prepared by solid state reaction of Si and WC at 1560 °C, with  $\text{NH}_4\text{HCO}_3$  as a pore generating agent. Phase composition, thermal expansion, flexural strength, and microstructure of the carbide ceramics were examined. Presence of the SiC, WC and  $\text{WC}_{1-x}$  phases were detected in the carbide ceramics. As Si content increased from 2 to 14 wt%, the coefficient of thermal expansion first decreased and then increased, with a minimum of  $4.11 \times 10^{-6} \text{ }^\circ\text{C}^{-1}$  at 8 wt% Si, whereas the flexural strength decreased gradually, from 143.9 to 82.7 MPa. Pores of SiC–WC ceramics were less than 2  $\mu\text{m}$  in diameter, because of the stacking interstice of carbide particles and volatilization of silicon. However in the presence of  $\text{NH}_4\text{HCO}_3$ , pores of SiC–WC ceramics were bimodally distributed, the stacking interstice of carbide particles loosened from 1 to 4  $\mu\text{m}$  and pores larger than 5  $\mu\text{m}$  were also formed.

© 2009 Elsevier Ltd and Techna Group S.r.l. All rights reserved.

**Keywords:** A. Sintering; B. Porosity; C. Coefficient of thermal expansion; D. Carbide**1. Introduction**

Transition metal carbides have unique chemical and physical properties, such as good hardness, wear resistance [1,2], chemistry stability and high melting point, which make carbide ceramics useful for filter medium, fuel cell electrodes [3,4], catalysts [5], impact absorbing structures [6,7] and refractories [8].

Multi-metal carbides composite was difficult to synthesize probably due to the poor wettability and thermal expansion matching among carbides [9]. Most of the studies on carbides so far have focused on monometallic carbides and cemented ceramics with a binder metal such as Co or Ni. Due to the lack of chemical resistance of cement carbide and relatively large thermal expansion of monometallic carbides, binder-less carbide composites [10,11] especially porous binder-less carbide composites with low thermal expansion ceramics have attracted great interest.

In this paper, porous SiC–WC composite ceramics with low thermal expansion coefficient were synthesized at relative low temperature (1560 °C) in a reducing atmosphere and their crystal phase, thermal expansion, flexural strength, and

microstructure were investigated as well as the influence of Si and  $\text{NH}_4\text{HCO}_3$ .

**2. Experimental**

WC (>99.9%, 1–2  $\mu\text{m}$ , China) and Si (>99.9%, 200# mesh, China) were used as raw materials and ammonium bicarbonate (Analytical reagent, China) as a pore generating agent (PGA). The weight percentage of Si was increased gradually from 2 to 16 wt%, the ammonium bicarbonate ranged from 0 to 20 wt% with constant 8 wt% Si. The batches were mixed for 20 min using a triturator and pressed into samples in moulds of  $\phi 20 \text{ mm} \times 3 \text{ mm}$  and  $5 \text{ mm} \times 5 \text{ mm} \times 40 \text{ mm}$  respectively. The samples were firstly placed in a muffle furnace at 190 °C for 3 h, which made the PGA decompose completely, and then sintered in an electric furnace at 1560 °C for 3 h in a closed alumina crucible with samples covered with graphite powder (200# mesh).

The crystal phases of the sintered ceramic samples were analyzed by a Philips PW1710 diffractometer with  $\text{Cu K}\alpha$ , 40 kV. The X-ray diffraction (XRD) pattern was recorded with a step size of  $0.02^\circ$  from  $15^\circ$  to  $90^\circ$  at the speed of  $4^\circ/\text{min}$ . The coefficient of thermal expansion (CTE) was measured in Ar atmosphere from 20 to 820 °C at a heating rate of  $20^\circ\text{C}/\text{min}$  (dilatometer GWP-1000 China). At least 10 sintered sample bars,  $5 \text{ mm} \times 5 \text{ mm} \times 40 \text{ mm}$  in size, for each composition

\* Corresponding author. Tel.: +86 411 84707182; fax: +86 411 84707182.

E-mail address: [ljf@dlut.edu.cn](mailto:ljf@dlut.edu.cn) (J. Li).

were tested for three-point bending strength, with a bend span of 30 mm and a crosshead speed of 0.1 mm/min. The microstructure of samples was observed by scanning electron microscopy (SEM) with a FEL Quanta 200 microscope operated in high vacuum and 20 kV.

### 3. Results and discussions

#### 3.1. Crystal phases of SiC–WC ceramics

The XRD patterns of sintered carbide ceramics composed of 8 and 14 wt% Si are shown in Fig. 1. The crystal structure of the carbides composite was characterized as hexagonal WC and SiC at Si < 8 wt%. No peaks of silicon were present in the SiC–WC material after sintering, indicating it totally transformed into SiC at low Si addition. A cubic  $WC_{1-x}$  phase was observed at Si > 8 wt%, regardless of the sintering ramps. This indicates that when  $T > 1400^\circ\text{C}$ , the transition of Si to SiC occurred preferentially, which may be attributed to the low melting point of silicon. With Si content increasing, more carbon atoms reacted with deposited Si on the surface of WC, which caused the lack of carbon in WC and the formation of  $WC_{1-x}$ .

#### 3.2. Linear thermal expansion and flexural strength of carbide ceramics

Fig. 2 shows the influence of silicon content on the thermal expansion coefficient (CTE) of SiC–WC ceramics. The thermal expansion coefficients first decreased to a minimum,  $4.11 \times 10^{-6}/^\circ\text{C}$  at Si = 8 wt% and then increased sharply as Si increased from 8 to 14 wt%.

The CTE of SiC–WC composite carbide ceramics depends on the CTE of SiC and WC. When silicon < 8 wt%, it vaporized, deposited and reacted with carbon at high temperature, and  $\beta$ -SiC was formed on the surface of WC grain. Being the average CTE of Si and  $\beta$ -SiC from 25 to  $1000^\circ\text{C}$  of  $4.2 \times 10^{-6}$  and  $3.8 \times 10^{-6}/^\circ\text{C}$  respectively, i.e. much lower than WC,  $5.2 \times 10^{-6}/^\circ\text{C}$ , the CTE of SiC–WC

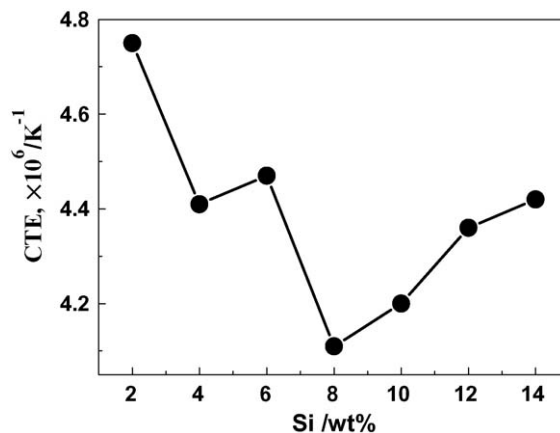


Fig. 2. The influence of silicon on CTE of SiC–WC composite ceramics.

decreased slightly with increasing silicon content and reached a minimum of  $4.11 \times 10^{-6}/^\circ\text{C}$  at 8 wt% Si. When the silicon content was over 8 wt%, the new phase  $WC_{1-x}$  formed, possessing CTE of  $8.1 \times 10^{-6}/^\circ\text{C}$ , when  $X = 0.5$  [12], i.e. much higher than SiC and WC. So the CTE of SiC–WC and internal stress increased sharply at increasing  $WC_{1-x}$ . At Si > 16 wt%, disruption of the ceramic occurred.

Pure WC particles were hard to be sintered at  $1560^\circ\text{C}$ . Herein the silicon was carbonized into low thermal expansion SiC, which had the proper thermal expansion matching with WC and increased the strength of composite carbide ceramics.

The influence of silicon on the flexural strength and the apparent porosity of composite carbide ceramics are shown in Fig. 3. The apparent porosity increased from 17.3 to 37.4% and the flexural strength decreased from 143.9 to 82.7 MPa, as silicon increased from 2 to 14 wt%. It indicated that parts of silicon volatilized but did not deposit on tungsten carbide grains to form SiC during sintering, which resulted in the increase in apparent porosity. The flexural strength was found to depend on the apparent porosity, and also decreased as silicon increased. Despite the apparent porosity reached 36% when silicon content was 14 wt%, the flexural strength was still higher than 80 MPa.

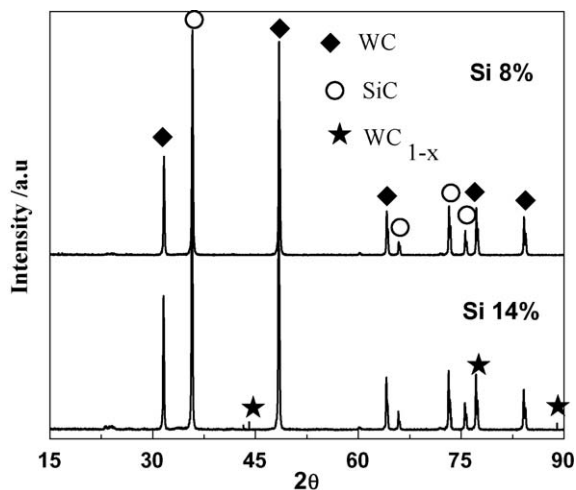


Fig. 1. XRD pattern of SiC–WC composite ceramics (8 and 14 wt% Si).

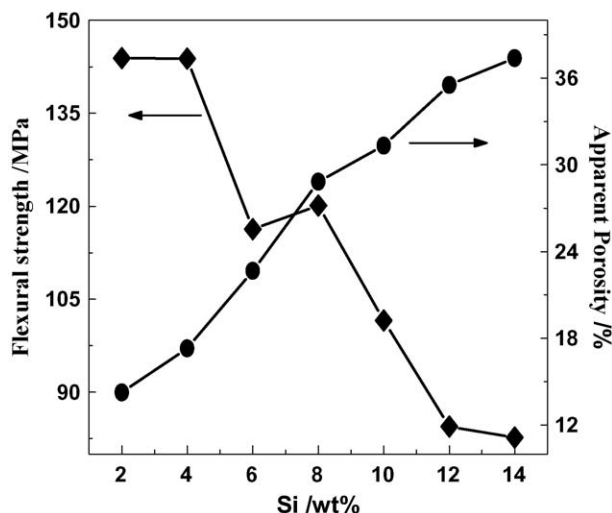


Fig. 3. The influence of silicon on flexural strength and apparent porosity.

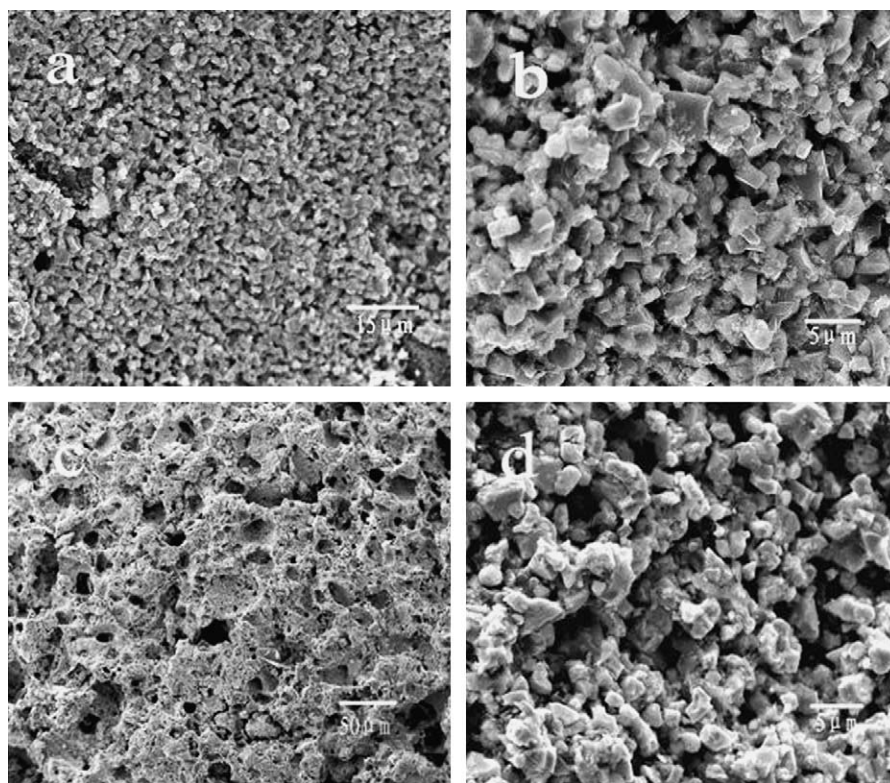


Fig. 4. SEM micrographs of SiC–WC ceramics (a and b) and SiC–WC–PGA ceramics (c and d).

### 3.3. Microstructure of porous SiC–WC composite ceramics

Representative SEM micrographs of the porous composite carbide ceramics (Si, 8 wt%) without ammonium bicarbonate are presented in Fig. 4(a and b). WC particles were uniformly distributed with average diameter of 1.5 μm, and rounded corners caused by silicon carburization. Presence of pores with radius < 1 μm was due to the stacking interstice of SiC–WC particles. Pores with radius > 1 μm might be a channel for silicon volatilization, see Fig. 4(a and b). SEM images of porous composite carbide (Si, 8 wt%) with ammonium bicarbonate (10 wt%) are shown in Fig. 4(c and d). Due to the  $\text{NH}_4\text{HCO}_3$  decomposition, connected pores larger than 5 μm in radius were observed. Meanwhile, the stacking interstices of SiC–WC grain loosened from 1 to 4 μm.

## 4. Conclusions

SiC–WC ceramics were prepared by solid state reaction between Si and WC at 1560 °C in a reducing atmosphere. When silicon content was less than 8 wt%, SiC and WC phases were present and the thermal expansion of the composite ceramics decreased to a minimum of  $4.11 \times 10^{-6}/^\circ\text{C}$  with 8 wt% silicon. With silicon > 8 wt%,  $\text{WC}_{1-x}$  phase appeared and the thermal expansion coefficient increased sharply as silicon content increases. As the silicon content rose from 2 to 14 wt%, the apparent porosity increased from 14.3 to 37.4%, and the flexural strength decreased from 143.9 to 82.7 MPa.

In porous SiC–WC ceramics, WC particles were uniformly distributed. Pores with average diameter of 1.5 μm were formed by stacking the interstice of carbide particles and Si evaporation. When  $\text{NH}_4\text{HCO}_3$  was added as a pore generating agent, pore radius increased to over 5 μm as a consequence of the interval and the stacking interstice of carbide particles.

## References

- [1] P.V. Krakhmalev, T. Adeva Rodil, J. Bergström, Influence of microstructure on the abrasive edge wear of WC–Co hardmetals, *Wear* 263 (2007) 240–245.
- [2] S.C. Zhang, G.E. Hilmas, W.G. Fahrenholtz, Zirconium carbide–tungsten cermets prepared by in situ reaction sintering, *Journal of the American Ceramic Society* 90 (2007) 1930–1933.
- [3] C.J. Barnett, G.T. Burstein, A.R.J. Kucernak, et al., Electrocatalytic activity of some carburised nickel, tungsten and molybdenum compounds, *Electrochimica Acta* 42 (15) (1997) 2381–2388.
- [4] M. Nagai, M. Yoshida, H. Tominaga, Tungsten and nickel tungsten carbides as anode electrocatalysts, *Electrochimica Acta* 52 (17) (2007) 5430–5436.
- [5] M.K. Neylon, S. Choi, H. Kwon, et al., Catalytic properties of early transition metal nitrides and carbides: n-butane hydrogenolysis, dehydrogenation and isomerization, *Applied Catalysis A: General* 183 (1999) 253–263.
- [6] K. Prabhakaran, Anand Melkeri, N.M. Gokhale, et al., Preparation of macroporous alumina ceramics using wheat particles as gelling and pore forming agent, *Ceramics International* 33 (2007) 77–81.
- [7] H. Chhina, S. Campbell, O. Kesler, Thermal and electrochemical stability of tungsten carbide catalyst supports, *Journal of Power Sources* 164 (2007) 431–440.

- [8] R. Koc, J.S. Folmer, Carbothermal synthesis of titanium carbide using ultrafine titania powders, *Journal of Materials science* 32 (1997) 3101–3111.
- [9] S. Chouzier, P. Afanasiev, M. Vrinat, et al., One-step synthesis of dispersed bimetallic carbides and nitrides from transition metals hexamethylenetetramine complexes, *Journal of Solid State Chemistry* 179 (2006) 3314–3323.
- [10] J.H. Liversage, D.S. McLachlan, I. Sigalas, Microstructure, phase and thermoelastic properties of laminated liquid-phase-sintered silicon carbide–titanium carbide ceramic composites, *Journal of the American Ceramic Society* 90 (2007) 2189–2195.
- [11] F. Akhtar, I.S. Humail, S.J. Askari, et al., Effect of WC particle size on the microstructure, mechanical properties and fracture behavior of WC–(W, Ti, Ta) C–6 wt% Co cemented carbides, *International Journal of Refractory Metals and Hard Materials* 25 (2007) 405–410.
- [12] A.W. Weimer, *Carbide nitride and boride material synthesis and processing*, Chapman and Hall, UK, 1997.